GBT MEMO 202

2-D phase closure with GBT laser rangefinders

Don Wells* D.Parker Michael Goldman Dana Balser Ray Creager
John Shelton Brian Ellison

December 3, 1999

Abstract

A phase closure experiment with nine laser rangefinders in a plane was performed on 1999-06-23. More than 5000 ranges were measured by the instruments in a period of about 2.5 hours. After extensive editing and iterative rejection operations, about 850 of these ranges have been adjusted in a least-squares fit which solves for station coordinate and refractivity corrections. The overall weighted RMS range residual from the fit is about 180 μm, which constitutes proof that the total system of atmosphere plus rangefinder hardware plus software reduction model is able to produce self-consistent geometric results to this accuracy. This is several times larger than the expected level of instrumental noise for the GBT rangefinders; the difference is presumed to be due to (as-yet unmeasured) $\approx \pm 125\,\mu$m deviations of the zero- and back-prism offsets from their design values.

Contents

1 About the experiment **2**

2 Rangefinder problems on 99-06-23 **3**

2.1 Cycle ambiguities & bad ranges 3

2.2 Internal phase (in)stability 4

2.3 Transmitter-to-detector leakage 6

3 Initial adjustment of monument and refractivity corrections **8**

4 Second adjustment of monument and refractivity corrections **16**

5 Conclusions & recommendations **26**

Bibliography **27**

*mailto:dwells@nrao.edu

1 About the experiment

On Wednesday 1999-06-23 nine rangefinders mounted on piers at 120 meter radius from the GBT pintle bearing were used to measure sets of ranges to each other's backprisms. During a period of about 2.5 hours a total of 78 2-minute cycles of such measurements were made. There were two sets of measurements, the first with 46 cycles and the second with 32 cycles. Of the nine rangefinders (see Figure 1 [p.2]), one (ZY101) was measured by seven other rangefinders. Two were measured six times, two were measured five times, two four times, and two rangefinders had three measurements. The minimum number of measurements for redundancy in a plane is three, so every rangefinder met this criterion for a 'phase closure' experiment, and five of the nine rangefinders were measured five or more times. Many paths were blocked, so we did not get the full $9 \times 8 = 72$ ranges per cycle; in practice we got roughly half that number per cycle. More than 5000 ranges were recorded.

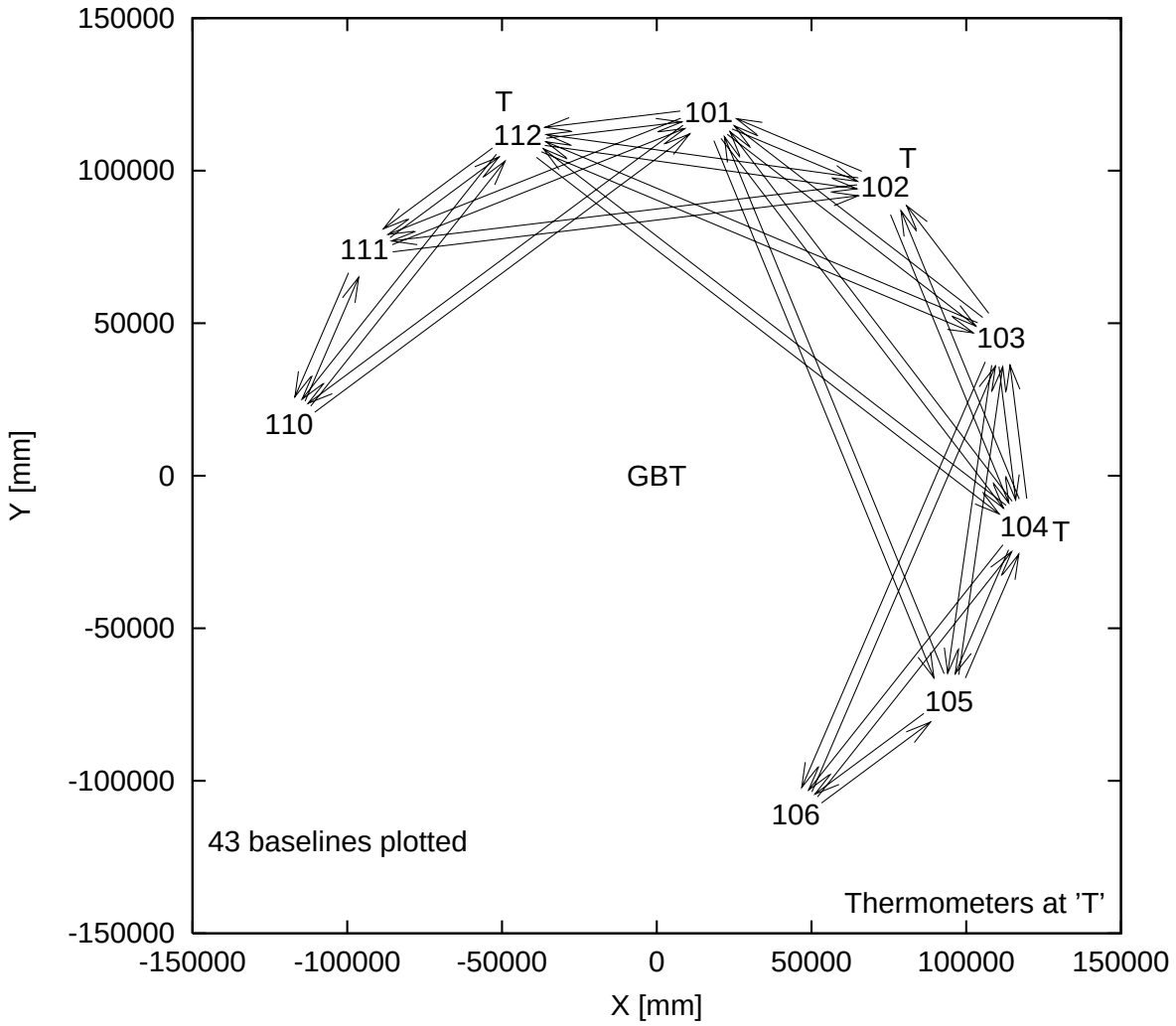

Figure 1: Baselines *before* initial adjustment (`pr[ranger,axis]` in Table 4 [p.14] & `r1+r2` in Table 6 [p.18])

The purpose of performing this type of experiment is to check whether the measurements over multiple redundant paths can be fitted to a model with acceptable residuals; this experiment is an end-to-end verification of the phase integrity of the entire rangefinder system, atmosphere plus electro-optical hardware plus data analysis software. There is a close analogy to the concept of "phase closure" in redundant aperture

```
# Now to check range to see if it agrees with a priori calculation
#                                        to within an acceptable tolerance:
$indexair = 1 + $refractivity{$scan} * 1e-6; # index of refraction in air
$indexbk7   = 1.527463;                      # index in prism glass
$halflambda = 299792.458/1500.0/2;      # [mm] 1.5_GHz half-lambda in vacuo
$tolerance  = 4.0;                      # [mm] cycle ambiguity tolerance
$rangecycle = $halflambda / $indexair;
$sum = 0; for ($i = 0; $i < 2; $i++) {       # Compute geometric distance:
    $k1 = $r1."_".$i; $k2 = $r2."_".$i;
    $sum += ($pr{$k1} - $pr{$k2})**2;
}
$computed = sqrt($sum)*$indexair             # Compute expected range:
            -$zerod{$r1}*$indexair -$zerop{$r1}*25.4*$indexbk7
            -$backd{$r2}*$indexair +$backp{$r2}*25.4*$indexbk7;
$diff = $rangeval - $computed;
if (abs($diff) > $tolerance) {
    for ($i = 1; $i < 3; $i++) {             # Test for cycle count errors:
        if (abs(abs($diff) - $i * $rangecycle) < $tolerance) {
            if ($diff > 0) { # Correct probable cycle count ambiguity:
                $rangeval += -$i*$rangecycle; $numcycle++; } else {
                $rangeval += +$i*$rangecycle; $numcycle++; }
            last;
        }
    }
}
if (abs($rangeval - $computed) > $tolerance) {
    $numdelete++; next; }                       # delete this rangeval
```

Figure 2: Algorithm to correct ranges for cycle ambiguities (coded in Perl [WCS96])

synthesis arrays, and so we will use that term to describe this experiment (*phase is the real observable in the rangefinder systems, so this term is entirely appropriate*). Certain other targets were measured during the experiment, but none of them achieved the redundancy necessary for a closure experiment, and they will not be discussed further here.

2 Rangefinder problems on 99-06-23

2.1 Cycle ambiguities & bad ranges

Cycle ambiguities and erroneous ranges are pervasive in the rangefinder datasets acquired on 99-06-23. The range periodicity is the group wavelength in air of the laser modulated at 1500 MHz, which is $\lambda_{\rm air} = \frac{c}{n_g f}$ [Par99, Eq.1.27,p.6], where n_g is the group refractive index [Par99, Sec.1.4,p.4]. Note the calculation of `rangecycle` in Figure 2, which includes n_g. The `refractivity` is of order 250, so `rangecycle` differs by less than 0.1% from the vacuum group wavelength (`halflambda` in Figure 2) which is simply the velocity of light times the refractive index divided by twice the 1.5 GHz laser modulating frequency:

$$\lambda_{\rm vacuo} = \frac{c}{2f} = \frac{299792458000}{2 \times 1500000000} = 99.93082\,{\rm mm}. \tag{1}$$

The fact that the modulation period of the GBT rangefinders is 100 mm to an accuracy of about 0.1% is convenient when inspecting listings of raw data of ranges measured over reciprocal paths: the cycle ambiguities are obvious. The AWK program [AKW88] `rfpcPlane4GetData.awk` reformatted the rangefinder data and separated the target retroreflector, ZRG and WEATHER data into separate files for the two runs.

The files were concatenated and then Perl [WCS96] program `rfpcPlane4FilterData.pl` performed the cycle ambiguity test (see Figure 2). The cycle test also tested residuals from predicted ranges, and deleted measurements whose residuals were larger than a certain tolerance. The tolerance is generous in this initial test because the provisional monument coordinates have errors of order 1 mm, so that ranges between them might have initial residuals of order 2 mm. Portions of the dataset which passed these tests are shown in Table 1 [p.7], and statistics of the tests are shown in Table 2 [p.8].

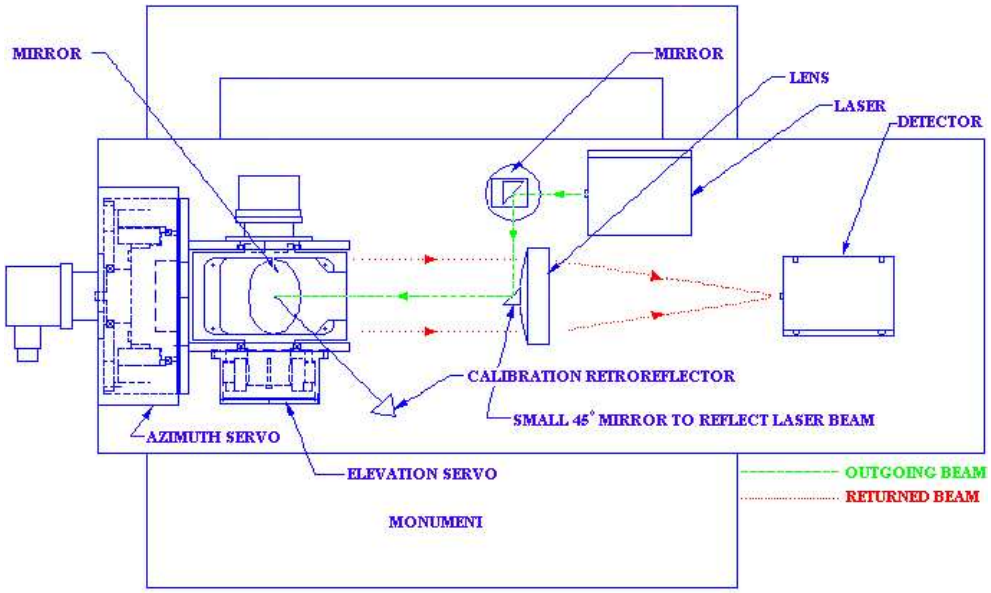

Figure 3: Rangefinder from above, showing "ZRG" prism (the "Calibration Retroreflector")

2.2 Internal phase (in)stability

Figure 3 shows a "calibration retroreflector" which is mounted on each of the rangefinders. The scan mirror can point the beam at this prism in order to monitor changes in the internal phase of the rangefinder system. The figure shows the prism off to one side of the main optical path, but the current production instruments actually have it mounted in the baseplate directly under the scan point of the mirror. These prisms are referred to as "ZRG" prisms in the rangefinder software. Each 2-minute measurement cycle included one measurement of each ZRG by its rangefinder. The resulting phases were subtracted from all target phases by the rangefinder's "ZIY" software [Cre98].

The ZRG measurements were logged by the ZIY software. Most of the rangefinders showed slow thermal drifts in their zero points, but three of them showed conspicuous instabilities in their zero points. In Figure 4 [p.5] we show the differences between successive ZRG measurements divided by the time between the measurements for each of the rangefinders. This is a plot of the time history of the *rate of change of internal phase* in the rangefinder systems. Horizontal lines are drawn to indicate rates of $+10\,\mu$m/min, 0 and $-10\,\mu$m/min. We can see that six of the rangefinders (101, 102, 103, 104, 106, 111) display noise of ± 5 to $\pm 10\,\mu$m/min in 2-minute samples about mean rates typically in the range $\pm 15\,\mu$m/min. The mean rates of some instruments are fairly constant during the 2.5 hours, but the mean rates of some instruments vary and sometimes the rates change sign! If these changes were caused by thermal drifts it might be supposed that the rates of all instruments would have the same sign and would vary in approximately the same way as ambient temperature varies.

Three rangefinders (105, 110, 112) display much larger irregular changes of phase. In Figure 4 the largest excursions of phase rate have been bounded to prevent overlapping of plots. Note that rangefinder 102

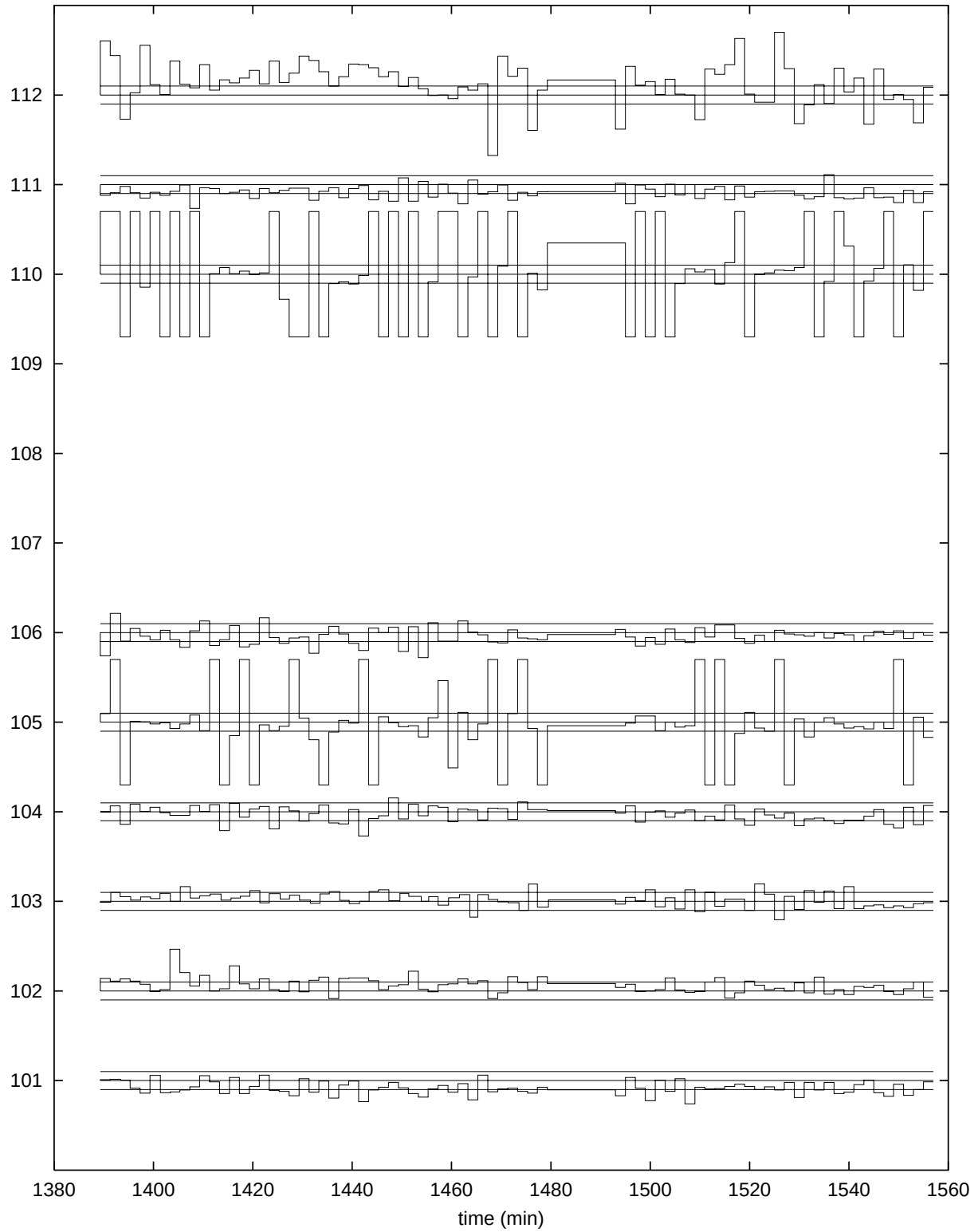

Figure 4: Rangefinder "ZRG" phase change rates [$\pm 10\,\mu$m/min indicated]

displays an unusually large phase change at about 1405 minutes; this may be an instance of the type of erratic behavior of the other three rangefinders. The large irregular phase changes in 105 and 110 caused substantial perturbations in the initial monuments-plus-refractivity-plus-prism-offset closure solutions which were reported informally to other GBT project personnel in July; at that time we characterized these solutions as demonstrating closure at the "5 ppm level" (0.5 mm in 100 m). At the time this was thought to reflect the overall system performance which had been achieved. Later it became clear that ZY105 and ZY110 had been operating *incorrectly* during the 06-23 experiment, and their data were given much lower weight. Solutions for prism offsets, monuments and refractivity after this reweighting had RMS fits of order $100\,\mu$m, which could be characterized as "demonstrating closure at the 1-ppm level", roughly the design goal of the rangefinder systems, but actually this conclusion was premature, because there was not sufficient data to support solving for so many unknowns in a proper, robust manner.

Rangefinder ZY102 has RMS range residual of $\approx 300\,\mu$m when measuring to ZY101 (see baseline 8 in Table 6 [p.18]); this large value is surprising because this combination gave the highest amplitude signal in this experiment. This is a saturation problem in the signal chain; amplitudes above 12 V are given lower weight in the current solutions to minimize its influence. Future versions of the rangefinder firmware should detect and flag this situation.

2.3 Transmitter-to-detector leakage

During the months after the 06-23 experiment the metrology group found that certain rangefinders had significant leakage from their transmitter circuits to their detector circuits. Such leakage of 1500 MHz transmitter signal will cause a rangefinder to indicate some phase (corresponding to a fictitious range) even when no signal is being detected due to light returned from a retroreflector. This leakage will also cause a phase bias (range error) when it mixes with returned-light signal. The extreme case is when the leakage is in quadrature with the signal. In that case, the phase error is [Par99, Sect.5.3.1]

$$\Delta\phi = \arctan(\frac{\text{leakage}}{\text{signal}}). \tag{2}$$

The corresponding distance error would be

$$\Delta R = (\frac{c}{2n_g f})\frac{1}{2\pi}\arctan(\frac{\text{leakage}}{\text{signal}}) \tag{3}$$

For example, if the leakage-to-signal ratio is 0.001 (0.1%) and $f = 1.5$ GHz, we will have

$$\Delta R = \frac{300000 \times 10^9}{2 \times 1 \times 1.5 \times 10^9} \times \frac{0.001}{6.28} = 100000 \times 0.000159 = 15.9\,\mu\text{m} \tag{4}$$

To prevent this problem from unduly influencing the closure experiment, ranges with lower amplitudes (larger leakage ratios) will be given larger a priori variances (lower weights). Examination of the instruments during the weeks following this experiment disclosed leakage levels as high as 8 mV in the rangefinders. For this experiment we choose to limit the range error to $\approx 100\,\mu$m, and so the limiting leakage ratio will be $\frac{15.9\times1000}{100} = 159$; for 8 mV leakage this implies larger sigmas for amplitudes below ≈ 1.3 V (in the code this is expressed as 4 mV and 50 μm; see the "*leakage*" entries in the statistical summary shown in Table 2 [p.8]).

The ZIY software has been changed since 99-06-23 to include a command which points the beam at the sky so that the leakage can be measured, and the instruments have been adjusted to minimize the leakage, which is now less than ≈ 2 mV. Even at this low level, leakage will still corrupt the phases of measurements which have amplitudes sufficient for good phase (range) determination, and therefore *this leakage must be compensated in all future work with these instruments.* Measurements of both ZRGs and targets include this leakage as a (complex) added signal; it follows that the amplitude and phase of the leakage signal should be measured separately (using the new ZIY command) so that they can be subtracted from the amplitude and phase of the ZRG and target measurements separately using complex arithmetic.[1] Then the ZRG phase can be subtracted from the target phase without a leakage contribution to the phase.

[1] Transform back to the measured amplitudes ($a = A\cos\phi, b = A\sin\phi$), and subtract as $z_1 - z_2 = (a_1 - a_2, b_1 - b_2)$.

Range data, with residuals from model fit						
`scan`	`r1`	`r2`	`ampl` Volts	`range` mm	$\sigma^2_{\texttt{range}}$ mm^2	$\Delta_{\texttt{range}}$ mm
101	101	102	11.63	61864.56	0.0025	-0.10
101	102	101	12.53	61864.81	1.0000	0.24
102	101	102	11.82	61864.56	0.0025	-0.06
102	102	101	12.43	61865.08	1.0000	0.55
103	101	102	11.86	61864.56	0.0025	-0.07
103	102	101	12.32	61865.28	1.0000	0.74
104	101	102	11.88	61864.59	0.0025	-0.04
105	102	101	12.46	61864.99	1.0000	0.44
106	101	102	11.88	61864.55	0.0025	-0.17
106	102	101	12.51	61864.82	1.0000	0.20
107	101	102	10.84	61864.60	0.0025	-0.06
107	102	101	12.30	61865.21	1.0000	0.64
108	101	102	11.85	61864.59	0.0025	-0.05
109	102	101	12.48	61864.99	1.0000	0.40
110	101	102	11.39	61864.56	0.0025	-0.09
110	102	101	12.38	61865.26	1.0000	0.71
(Many lines omitted to fit page)						
132	101	111	5.07	119770.77	1.0000	0.01
132	111	101	5.45	119770.18	1.0000	-0.43
133	101	111	4.82	119770.78	1.0000	-0.01
133	111	101	5.43	119770.20	1.0000	-0.44
134	101	111	3.44	119770.76	1.0000	-0.02
134	111	101	4.59	119770.16	1.0000	-0.47
136	101	111	3.99	119770.77	1.0000	0.14
136	111	101	4.93	119770.22	1.0000	-0.26
137	101	111	3.22	119770.76	1.0000	-0.03
137	111	101	5.38	119770.21	1.0000	-0.43
138	101	111	3.65	119770.81	1.0000	0.01
138	111	101	5.54	119770.24	1.0000	-0.40
139	101	111	4.57	119770.84	1.0000	0.02
139	111	101	5.09	119770.33	1.0000	-0.34
140	101	111	3.81	119771.00	1.0000	0.11
141	111	101	5.02	119770.34	1.0000	-0.27
142	101	111	2.62	119771.04	1.0000	0.11
142	111	101	5.03	119770.43	1.0000	-0.35
143	101	111	3.11	119771.03	1.0000	0.08
143	111	101	4.84	119770.43	1.0000	-0.37
(Many lines omitted to fit page)						
228	112	111	3.50	61896.10	0.1600	0.23
229	111	112	0.07	61895.76	0.9297	0.21
229	112	111	3.20	61896.07	0.1600	0.15
230	111	112	0.08	61895.59	0.6246	-0.02
230	112	111	2.05	61896.10	0.1600	0.12
231	111	112	0.08	61895.72	0.7007	0.03
231	112	111	1.10	61896.17	0.1600	0.11
232	111	112	0.08	61895.56	0.5960	-0.06
232	112	111	3.65	61896.10	0.1600	0.10
233	111	112	0.08	61895.67	0.6159	0.12
233	112	111	4.10	61896.05	0.1600	0.12

Table 1: Portions of the observational data after input filtering (note variances σ^2_{range})

3 Initial adjustment of monument and refractivity corrections

Preliminary coordinates of the rangefinder monuments were previously determined by a survey using the Topcon[2] geodetic total station which NRAO owns; the survey was reduced using the STAR*NET[3] adjustment program. Although the Topcon has nominal accuracy specification 3 mm, the adjustment residuals indicated that the true accuracy is about 1 mm.

Ray Creager used the ZIY software display of scan mirror coordinates to get the scan mirror coordinates (monument coordinates plus Kelvin-mount-to-scan-mirror offset, the `pr` column of Table 4 [p.14]) which were used in this model fit to the range data.

The distance from the scan mirror to the ZRG calibration prism (Figure 3) produces a phase offset when the ZRG phase is subtracted from the range data, and this offset must be compensated. Unfortunately precise as-built values of these distances, which vary slightly from rangefinder to rangefinder, have not yet

[2]Topcon Corporation, 75-1 Hasunuma-cho, Itabashi-ku, Tokyo, 174-8580 Japan.
See `http://www.topcon.co.jp` and `http://www.topconlaser.com/home.htm`
[3]Starplus Software, Inc.

	Processing file `19990623.230916.DAT`	
2720	total input range measurements	
828	ranges deleted because `ZEG31020` or `REFLECTOR`	*no redundancy*
414	`ZRG` measurements processed	
45	`WEATHER` measurements processed	
798	ranges deleted because $A < 0.03$ V	*insufficient signal*
526	ranges have $\sigma = 1.0$ mm because $A > 12$ V	*too much signal*
241	ranges have $\sigma > 0.05$ mm because $A < 1.27235$ V	0.004 V *leakage*
107	ranges have $\sigma = 1.0$ mm because ZY105	*unstable phase*
108	ranges have $\sigma = 1.0$ mm because ZY110	*unstable phase*
249	ranges have $\sigma = 0.4$ mm because ZY112	*unstable phase*
277	ranges have $\sigma = 0.05$ mm (data believed OK)	
1508	ranges written by `rfpcPlane4GetData.awk`	
	Processing file `19990624.005257.DAT`	
2652	total input range measurements	
594	ranges deleted because `ZEG31020` or `REFLECTOR`	*no redundancy*
297	`ZRG` measurements processed	
32	`WEATHER` measurements processed	
1403	ranges deleted because $A < 0.03$ V	*insufficient signal*
88	ranges have $\sigma = 1.0$ mm because $A > 12$ V	*too much signal*
535	ranges have $\sigma > 0.05$ mm because $A < 1.27235$ V	0.004 V *leakage*
92	ranges have $\sigma = 1.0$ mm because ZY105	*unstable phase*
0	ranges have $\sigma = 1.0$ mm because ZY110	*unstable phase*
201	ranges have $\sigma = 0.4$ mm because ZY112	*unstable phase*
36	ranges have $\sigma = 0.05$ mm (data believed OK)	
952	ranges written by `rfpcPlane4GetData.awk`	
	Processing file `rfpcPlane4Merged.dat`	
2460	input range measurements read	
1809	cycle errors corrected (Figure 2)	
260	ranges deleted because $\lvert R_{\rm obs} - R_{\rm calc}\rvert > 4.0$ mm (Figure 2)	*obviously invalid*
2200	ranges written by `rfpcPlane4FilterData.pl`	

Table 2: Statistics of the filtering of the data used in the initial adjustment

ZRG and backprism calibrations & zero point corrections								
`ranger`	`zerod` mm	$\sigma^2_{\texttt{zerod}}$	`zerop` inch	`backd` mm	$\sigma^2_{\texttt{backd}}$	`backp` inch	`zeroc` mm	`backc` mm
101	120.65	0.09	0.7416	40.64	0.09	0.7371	0.00	0.00
102	120.65	0.09	0.7405	40.64	0.09	0.7406	0.00	0.00
103	120.65	0.09	0.7383	40.64	0.09	0.7380	0.00	0.00
104	120.65	0.09	0.7364	40.64	0.09	0.7365	0.00	0.00
105	120.65	0.09	0.7414	40.64	0.09	0.7399	0.00	0.00
106	120.65	0.09	0.7414	40.64	0.09	0.7411	0.00	0.00
110	120.65	0.09	0.7407	40.64	0.09	0.7375	0.00	0.00
111	120.65	0.09	0.7406	40.64	0.09	0.7420	0.00	0.00
112	120.65	0.09	0.7369	40.64	0.09	0.7360	0.00	0.00

Table 3: Zero- and back-prism offsets and heights

been measured.[4] Examination of the drawings D35420M008 (GBT Laser Ranging System Layout Drawing, revision E 95-09-18) and D35420M012 (GBT Laser Ranging System Az Base Mount, revision F 94-09-29) indicates that the distance is 4.7500 ± 0.0002 inch (120.650 ± 0.005 mm), assuming that the face of the prism is flush with the rangefinder baseplate. We use this number (`zerod` in Table 3 [p.9]) as the zero prism offset in the adjustment below.

A rangefinder can determine the distance from its scan mirror to the scan mirror of another rangefinder if the second rangefinder turns its scan mirror so that the rear side faces the first rangefinder. There is a "back prism" mounted behind each of the scan mirrors. Examination of the mechanical drawings indicates that the back prism is flush with a shoulder which is 1.600 inch (40.64 mm) from a shoulder which is intended to be flush with the scan mirror.[5] We use this number (`backd` in Table 3 [p.9]) in the adjustment below.

Several hours before the 06-23 experiment, Michael Goldman and Don Wells had a special plastic tool made in the GB machine shop,[6] and John Shelton used the tool to measure the zero prism offset of a sample rangefinder; he got 120.49 ± 0.13 mm, consistent with the design value reported above. He also measured the back prism offset of that sample rangefinder to be 40.65 ± 0.2 mm, again consistent with the design.

Each of the zero- and back-prisms has a "height" (distance from face to apex), which determines the time delay (phase) of the laser light when travelling from the face to the effective return point of the prism and back. These heights vary slightly from prism to prism, and they were obtained from the logbooks of prism calibrations so that they could be used in the adjustment below (see `zerop` and `backp` in Table 3 [p.9]).

Weather station data was logged during the two runs. In addition to pressure and humidity sensors, there were three thermometers associated with the rangefinders (see Figure 1 [p.2] for the geometry):

Sensor	Location
1	ZY104
2	ZY102
3	ZY112

[4] The answer to the obvious question is: "Yes, the offsets of the zero- and back-prisms of the instruments will be calibrated before the GBT becomes operational." Another error which must be calibrated is the de-centering of the laser spots on their scan mirrors. The "azimuth" and "elevation" axes of each rangefinder should intersect in a point which should be in the plane of the scan mirror and the laser beam should be circular and centered on that point; a beam centering error of order 25 μm will produce a range error of comparable magnitude. This instrument calibration work will a metrology laboratory activity for winter periods when field work is not practical. The ultimate objective of all such calibration work is to be able to replace an instrument and resume measurements by simply entering the instrument serial number in the ZIY file that identifies the instrument on each monument or feed arm location.

[5] Ron Taggert, private communication

[6] Done in less than three hours, from concept to finished device!

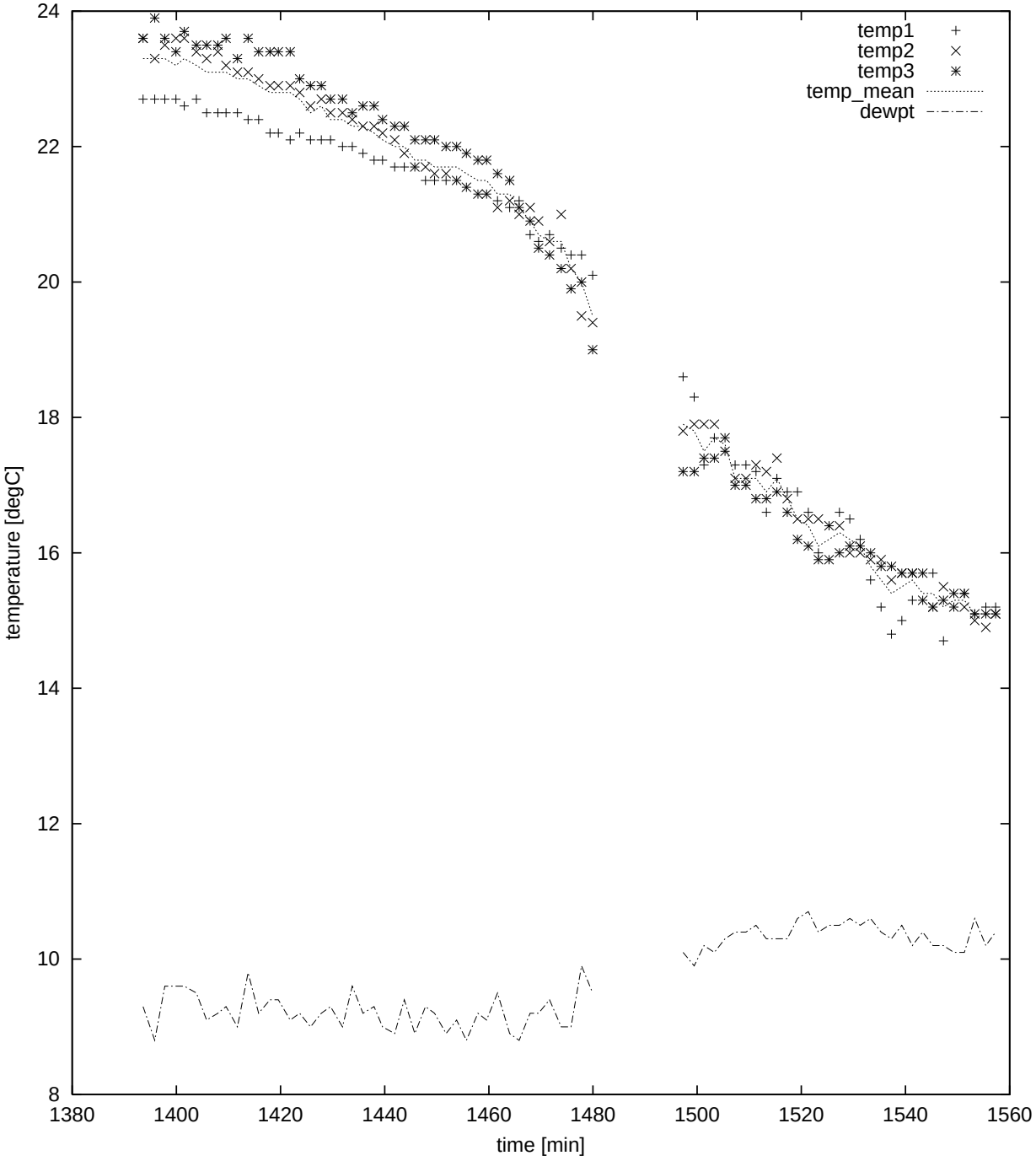

Figure 5: Air temperatures during the experiment

These thermometers are Omega ON-950-44033 thermistors, with a specification accuracy of ±0.1°C. The differences between them which are seen during tests (see Table 5 [p.15] and Figure 5 [p.10]) appear to reflect differences in temperature at the different sensor sites, possibly due to shading by the GBT. The refractivity values computed for each of them[7] were included in the data files for the experiment and were extracted during the input data processing. In the adjustments discussed below the mean of the three refractivity estimates ("`temp_mean`" in Figure 5 [p.10]) is used as the a priori estimate of refractivity ("predicted" in Figure 9 [p.21]), and a correction is produced for each 2-minute observation cycle (see `refractc` in Table 5 [p.15] and "adjusted" in Figure 9 [p.21]).

In the adjustment which follows we will compute corrections to the a priori estimates of refractivity, and will simultaneously adjust the rangefinder monument coordinates. Because range changes are proportional to refractivity changes, an unconstrained simultaneous adjustment must necessarily fail due to complete correlation between refractivity and the overall scale factor for monument coordinate changes. It is necessary to constrain some scale factor of the solution, and we do this by insisting that the adjusted distance between two of the monuments (ZY105 and ZY101, an arbitrary choice) will be held constant. The `range` value given below was computed from the `pr` values for ZY101 and ZY105 in Table 4 [p.14]:

Scale factor (expansion) constraint				
`scan`	`r1`	`r2`	`range` mm	$\sigma^2_{\texttt{range}}$ mm^2
0	101	105	207879.34	0.0001

The `scan` number of *zero* will be the signal that this fake observation should be applied as a constraint on the solution by the "`if(scan==0)`" test in Figure 6 [p.12]. Note that in the application of the constraint an additional small factor of order 10 ppm is applied to correct the inferred systematic error of the original Topcon survey so that the refractivity adjustment in Table 5 [p.15] will have approximately zero mean.

The Gaussfit [JFMM88] model which adjusted the monument coordinates and refractivity corrections using the rangefinder data is shown in Figure 6 [p.12]. It is based on the concepts developed in previous simulation work by one of us [Wel99], but includes a number of improvements. The physical and geometrical basis of the formulæ implemented in this model was reviewed extensively by the authors during the course of the analysis of the 99-06-23 data, and we believe it to be correct. The formulæ are based on discussions in reports by the GBT metrology group (e.g. [Gol98, Gol96, Par99]).

The model assumes a priori `constant` values for the coordinates `pr[,]` for each rangefinder, refraction estimates `refract[]` for each scan cycle (time), zero-prism calibrations `zerod[]` and `zerop[]` and back-prism calibrations `backd[]` and `backp[]`. It solves for (by declaring as `parameters`) the monument corrections `prc[,]` and the refraction corrections `refractc[]`. The 06-23 datasets had sufficient redundancy before they were filtered that they could also have supported solving for the `zeroc[]` and `backc[]` corrections (by declaring them as `parameter` rather than `constant`). However, we are forced to declare these corrections as `constant` because the large amount of corrupted data in the 06-23 datasets has reduced the redundancy to too low a level.[8] The independent variables of an observation (declared as `data` in Gaussfit) are the rangefinder `r1` (e.g. '103') which measures the `range` (the dependent variable, declared as `observation`) to rangefinder `r2` (e.g. '104') as part of a `scan` (e.g. '210'). Each such observation (a row in Table 1 [p.7])

[7] Refractivity varies by about 1 ppm per °C; see [Par99, Chapter 1] for full details and formulæ.

[8] The X and Y monument coordinate corrections are two unknowns for each of the nine rangefinders. The two prism corrections would be two more unknowns, for a total of $9 \times 4 = 36$ unknowns. The refractivity correction adds one more unknown for the 2-minute cycle. There are four constraints in the 2-D problem (see discussion elsewhere in this section), which deduct from the unknowns, giving a final total of $9 \times 4 + 1 - 4 = 33$ parameters to be determined in a 2-minute cycle. As we will see later (Table 6 [p.18]), only ≈ 30 baselines have significant weight after the filtering operations. We would have had 42 baselines if ZY105, ZY110 and ZY112 had not had phase instability problems, and we could have had as many as $9 \times 8 = 72$ baselines in principle. The minimum required redundancy in this problem is that the number of baselines exceed the effective number of parameters, and so we have fallen below the threshold. With the prism corrections declared as `constant`, we are solving for $9 \times 2 + 1 - 4 = 15$ parameters, and our ≈ 30 baselines will provide $\approx 2\times$ as many observations as parameters. Experience shows that a $2\times$ ratio will support robust least-squares solutions.

```
/* rfpcPlane4Model.gf --- rangefinders_in_plane & refractivity
   This model does a LS fit of inter-rangefinder measurements between
   N rangefinders in a plane with an effective index of refraction per
   'scan' (observation cycle).
   1999-06-29 --> 10-29: D.Wells, NRAO-CV, adapted from rfsPlane3Model.gf
*/
constant        pr[ranger,axis], refract[scan];
constant        zerod[ranger], zerop[ranger], backd[ranger], backp[ranger];
constant        backc[ranger];                    /* back prism corrections */
constant        zeroc[ranger];                    /* zero prism corrections */

parameter       refractc[scan];                   /* refraction corrections */
parameter       prc[ranger,axis];                 /* monument   corrections */
data            scan, r1, r2;
observation     range;
main() {
  variable nr, sumprc[2], sumangular, indexair, sum, i, indexbk7,
           pintle[2], computed, found, lr1[30], radius, cost, sint, da;

  nr=0;sumprc[0]=0;sumprc[1]=0;sumangular=0; pintle[0]=0;pintle[1]=0;
  while (import()) {          /* read scan,r1,r2,range for next observation */
    sum = 0; for (i = 0; i < 2; i = i + 1)
                sum = sum + ((pr[r1,i]+prc[r1,i]) - (pr[r2,i]+prc[r2,i]))^2;
    computed = sqrt(sum);
    if (scan==0) {     /* scan-zero ranges are used to constrain expansion: */
      exportconstraint(range - computed*(1+12.0e-6)); /* 12ppm Topcon error */
    } else {
      indexair = 1+(refract[scan]+refractc[scan])*1e-6;
      indexbk7 = 1.527463;
      computed = computed * indexair
               -(zerod[r1]+zeroc[r1])*indexair -zerop[r1]*25.4*indexbk7
               -(backd[r2]+backc[r2])*indexair +backp[r2]*25.4*indexbk7;
      export(range - computed);    /* eqn of condition for this observation */

      found=0; for (i=0; i<nr; i=i+1) { if (r1==lr1[i]) { found = 1; } }
      if (found == 0) {                           /* if r1 not seen, then */
        lr1[nr] = r1; nr = nr + 1;                /*   add r1 to our list */
        for (i = 0; i < 2; i = i + 1)             /* and form sums for r1 */
        sumprc[i] = sumprc[i] + prc[r1,i];            /* sum translations */
        sum = 0; for (i = 0; i < 2; i = i + 1)
        sum = sum + (pr[r1,i] - pintle[i])^2;
        radius = sqrt(sum);
        cost = (pr[r1,0] - pintle[0]) / radius;
        sint = (pr[r1,1] - pintle[1]) / radius;
        da = -prc[r1,0]*sint +prc[r1,1]*cost;
        sumangular = sumangular + (da / radius);          /* sum rotations */
      }
    }
  }
  for (i = 0; i < 2; i = i + 1)
      exportconstraint(sumprc[i]); /* constrain translation     of solution */
  exportconstraint(sumangular);    /* constrain rotation        of solution */
}
```

Figure 6: Gaussfit model for rangefinders-in-a-plane with refractivity corrections

becomes a single equation of condition in the least squares regression ("adjustment" in surveyor-speak) performed by Gaussfit.

The `while(import())` statement of the model reads the next observation. The geometric distance between adjusted monument coordinates is computed. If the scan number is zero, this distance is used to constrain the scale factor of the solution using the special fictitious observation. For all other observations the algorithm includes the refraction and prism contributions to the observed phase. The equation of condition for the observation is produced by the `export(range-computed)` (observed minus computed difference) statement; Gaussfit's goal is to adjust the variables declared as `parameter` so as to minimize the weighted[9] sum of the squares of these differences.

In addition to the scale factor constraint discussed above, the model implements three other constraints by forming three sums: `sumprc[0]`, `sumprc[1]` and `sumangular`. The monument corrections for each rangefinder are added to the `sumprc[]` values and the rotational component of these corrections about the pintle bearing is added to the angular sum. The last three lines of the model declare these sums as constraints (Gaussfit is required to adjust the `parameter` values such that the constrained expressions remain zero). These constraints are necessary because range data alone is invariant under translation and rotation, and so an unconstrained solution for the `prc[,]` parameters diverges to infinity. The translation constraint could be implemented by constraining the `prc[]` components of one rangefinder to zero; this works but is esthetically displeasing because the rangefinders are not treated identically (errors are not spread uniformly over the unknowns). Likewise, rotation could be constrained by constraining the sum of the ΔY corrections of two monuments widely separated in X (e.g., ZY104 and ZY110 in Figure 1 [p.2]); the `sumangular` algorithm implemented in Figure 6 [p.12] is more general. A 2-D solution requires four constraints (X-translation, Y-translation, [Z-]rotation and scale).[10]

[9] "By definition, the variances are the *squares* of the standard deviations, and are inversely proportional to the weights." [JFMM88, Sect.3.2.1] The estimated variances of the observed ranges are supplied to Gaussfit: $\sigma^2_{\rm range} = 0.0025\,{\rm mm}^2$ in Table 1 [p.7] is saying that $\sigma_{\rm range} = 50\,\mu$m. Observations in that table with variance 0.0025 will have 400× more weight in the solution than observations with variance estimated as 1.0000 ($\sigma_{\rm range} = 1\,$mm).

[10] A 3-D solution will require three more constraints (Z-translation, X-rotation and Y-rotation), for a total of seven.

Monument Adjustment					
ranger	axis	pr mm	$\sigma^2_{\mathtt{pr}}$	prc mm	$\sigma_{\mathtt{prc}}$ mm
101	0	16774.69	1	-0.05	0.02
101	1	118878.29	1	-1.36	0.04
102	0	73847.65	1	-0.15	0.02
102	1	94628.32	1	-0.00	0.03
103	0	111273.88	1	-0.56	0.04
103	1	44936.98	1	-0.63	0.02
104	0	118818.20	1	-1.03	0.03
104	1	-16660.16	1	0.06	0.01
105	0	94562.73	1	-0.25	0.05
105	1	-73898.37	1	1.25	0.01
106	0	44964.99	1	0.72	0.09
106	1	-111244.72	1	0.82	0.07
110	0	-118783.07	1	-0.03	0.10
110	1	16880.36	1	0.17	0.07
111	0	-94444.51	1	-0.01	0.04
111	1	74079.60	1	0.03	0.05
112	0	-44851.26	1	1.37	0.01
112	1	111355.86	1	-0.34	0.03

Table 4: Provisional monument coordinates and their initial adjustment (prc)

Table 4 [p.14] gives the adjustments to the monument coordinates which were produced in the initial solution. The formal errors of most of the prc values are less than 100μm, and the prc values themselves are of order 1 mm or less, consistent with the original Topcon survey.

Gaussfit also computed refractivity corrections, and these are tabulated in Table 5 [p.15]. These corrections have formal errors of 1 ppm or less; each such correction is based on the data from one 2-minute scan cycle. The temperatures were not measured for all scans; in particular, temperatures are not available at the start of the data acquisition runs, and so the estimated refractivity is set to 254, appropriate for 20°C. The refractc values for such cases demonstrate the power of the solution to compensate errors in the a priori estimated refractivity.

Refractivity corrections for 2-minute scans								
scan	temp1 °C	temp2 °C	temp3 °C	dewpt °C	press mbar	refract ppm	refractc ppm	$\sigma_{\texttt{refractc}}$ ppm
101	0.0	0.0	0.0	0.0	0.0	254.0	-4.0	0.2
102	0.0	0.0	0.0	0.0	0.0	254.0	-4.7	0.3
103	22.7	23.6	23.6	9.3	925.8	248.5	1.0	0.3
104	22.7	23.3	23.9	8.8	925.8	248.5	1.0	0.3
105	22.7	23.5	23.6	9.6	925.8	248.5	1.2	0.3
106	22.7	23.6	23.4	9.6	925.8	248.5	2.4	0.3
107	22.6	23.6	23.7	9.6	925.8	248.5	1.5	0.4
108	22.7	23.4	23.5	9.5	925.7	248.6	1.1	0.3
109	22.5	23.3	23.5	9.1	925.7	248.6	1.8	0.2
110	22.5	23.4	23.5	9.2	925.8	248.6	1.1	0.3
111	22.5	23.2	23.6	9.3	925.7	248.6	-0.4	0.4
112	22.5	23.1	23.3	9.0	925.7	248.8	1.0	0.3
(Some lines omitted to fit page)								
202	0.0	0.0	0.0	0.0	0.0	254.0	0.6	0.5
203	18.6	17.8	17.2	10.1	926.1	253.2	1.0	0.5
204	18.3	17.9	17.2	9.9	926.1	253.2	2.5	0.5
205	17.3	17.9	17.4	10.2	926.0	253.4	-1.6	0.6
206	17.7	17.9	17.4	10.1	926.0	253.3	-1.6	0.7
207	17.7	17.7	17.5	10.3	926.0	253.4	-1.6	0.6
208	17.3	17.1	17.0	10.4	926.1	253.8	-1.4	0.6
209	17.3	17.1	17.0	10.4	926.1	253.8	-2.2	0.6
210	17.2	17.3	16.8	10.5	926.1	253.9	-1.7	0.7
211	16.6	17.2	16.8	10.3	926.2	254.0	0.3	0.8
212	17.1	17.4	16.9	10.3	926.2	253.8	0.6	0.5
213	16.9	16.8	16.6	10.3	926.2	254.2	-2.1	0.6
214	16.9	16.5	16.2	10.6	926.2	254.4	1.3	0.6
215	16.6	16.5	16.1	10.7	926.3	254.5	-2.8	0.7
216	16.0	16.5	15.9	10.4	926.3	254.8	2.2	0.6
217	16.4	16.4	15.9	10.5	926.3	254.6	-0.2	0.5
218	16.6	16.4	16.0	10.5	926.3	254.6	-2.4	0.8
219	16.5	16.0	16.1	10.6	926.4	254.7	-0.7	0.8
220	16.2	16.0	16.1	10.5	926.3	254.8	0.2	0.5
221	15.6	15.9	16.0	10.6	926.4	255.0	-1.7	0.7
222	15.2	15.9	15.8	10.4	926.4	255.2	-2.3	0.6
223	14.8	15.6	15.8	10.3	926.4	255.5	-0.9	0.8
224	15.0	15.7	15.7	10.5	926.5	255.4	-0.8	0.8
225	15.3	15.7	15.7	10.2	926.5	255.3	1.7	0.6
226	15.3	15.3	15.7	10.4	926.4	255.4	-0.2	0.8
227	15.7	15.2	15.2	10.2	926.5	255.5	-1.8	0.7
228	14.7	15.5	15.3	10.2	926.5	255.7	-2.0	0.8
229	15.2	15.2	15.4	10.1	926.5	255.6	-1.1	0.8
230	15.4	15.2	15.4	10.1	926.5	255.5	-0.0	0.9
231	15.1	15.0	15.1	10.6	926.5	255.7	1.0	0.5
232	15.2	14.9	15.1	10.2	926.5	255.8	-0.1	1.1
233	15.2	15.1	15.1	10.4	926.6	255.7	-1.1	0.7

Table 5: Temperatures and refractivity, initial refractivity corrections

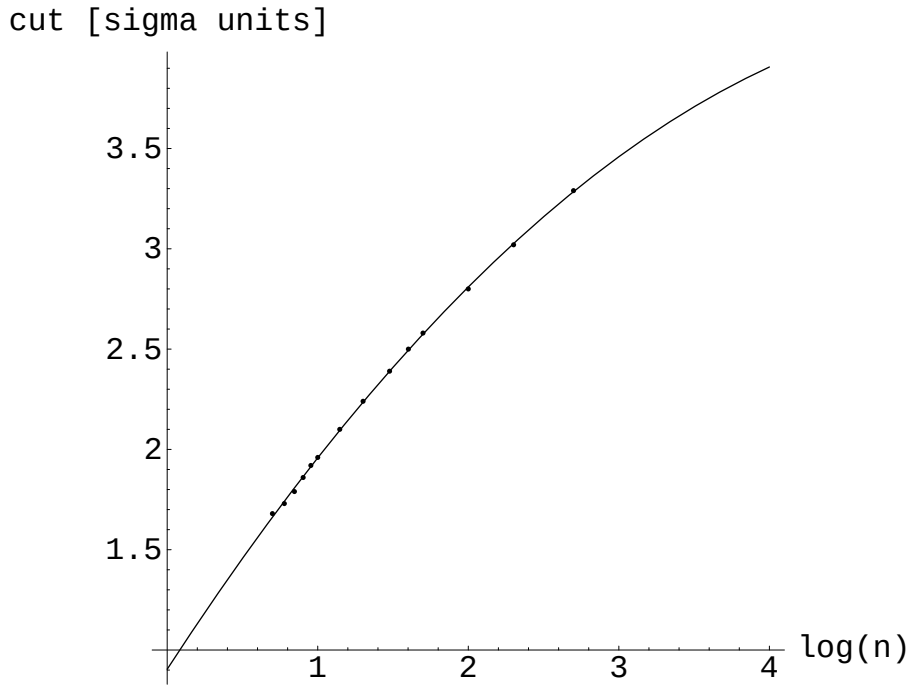

Figure 7: Chauvenet rejection rule as function of sample size [Par61, p.177]

4 Second adjustment of monument and refractivity corrections

The monument solution in Table 4 [p.14] and refractivity solution in Table 5 [p.15] are perturbed by "outlier" (large residual) observations. The initial data filter tests have excluded many outliers (see Table 2 [p.8]), but some remain. We can detect these by examining the range residuals (Δ_{range} in Table 1 [p.7]) on a per-baseline basis. In Table 6 [p.18] we tabulate the 43 combinations of `r1` and `r2` which occur in the 06-23 dataset after the initial data filtering. The n column is the number of ranges available for each baseline, and n' is the number that remain after `iters` cycles of iterative rejection produce the mean residual $\overline{\Delta R}$. The iterative rejection algorithm computes a standard error $\sigma_{\overline{\Delta R}}$ about $\overline{\Delta R}$ on each cycle. It then rejects any residual whose absolute value exceeds $k\sigma$. The value of k is recomputed after each cycle using the Chauvenet rule (Figure 7), as the sample size decreases due to rejection. The formula for k is (in AWK):

```
function chauvenet(n)
{
    x = n;
    if (x < 5) x = 5;
    x = log(x) / log(10);
    return(0.904321 +1.15484*x -0.101086*x^2);
}
```

The concept of Chauvenet's criterion for rejection is that "a measurement in a set of n trials shall be rejected if its deviation (reckoned from the mean) is such that the probability of occurrence of all deviations equally large or larger does not exceed $1/(2n)$."[Par61, p.176] If the distribution is normal (Gaussian) and there are only a modest number of outliers, the iterative rejection algorithm generally converges robustly to the mean and standard deviation of the normal part of the distribution. However, the reader should be aware that if the distribution is bimodal or has a significant uniform component, the algorithm may be unable to reject the outliers and converge to the mean of the primary normal distribution component. A good example occurs in our final histogram plot Figure 10 [p.24], where baseline 30 (ZY112↦ZY102), with 48 ranges, appears to be a composite distribution, with a normal component and an approximately uniform component; the relative sizes of the two components are such that the algorithm has not been able to reject the uniform component, and the mean (halfway between the $\pm\sigma$ bars) is perturbed by more than $100\,\mu$m from the normal component.

The mean signal level $\overline{\texttt{ampl}}$ and mean range $\overline{R}$ are tabulated as an aid for interpretation of the residuals. It is obvious that this initial adjustment displays essentially *no* correlation of residual amplitudes with either signal level or range. The sums of relative statistical weight[11] $\sum w$ for the baselines are determined by the RMS values assigned by `rfpcPlane4GetData.awk` (Figure 2 [p.8]) and the number of observations per baseline; note that a range with $\sigma = 50\,\mu$m has $400\times$ more weight than a range with $\sigma = 1\,$mm ($1000\,\mu$m).

The final line of the table (`baseline`=0) gives the mean residual for the set of range measurements after iterative rejection ($\overline{\Delta R}$ and n' for baseline 0) plus the standard deviation of the distribution of residuals about that mean ($\sigma_{\overline{\Delta R}}$ for baseline 0). This leads to a conclusion:

> The initial adjustment of monument and refractivity corrections using about 2000 of the ranges acquired 99-06-23 can be summarized by saying that it demonstrates phase closure with a weighted RMS of about $190\,\mu$m.

However, the large range of the $\overline{\Delta R}$ values, and the fact that they often greatly exceed their $\sigma_{\overline{\Delta R}}$ values, is hinting that phase closure in the initial adjustment is still somewhat limited by outliers in the distribution of range residuals. The next round of data filtering depends on four assumptions:

- there really is a solution to the problem (i.e., the instruments worked correctly for a substantial fraction of the observing time and we have a correct software implementation of the correct physical model).
- when the instruments operate correctly, ranges have an approximately normal (Gaussian) distribution.
- the initial adjustment of monument coordinates has bounded the absolute values of the monument position errors to about $200\,\mu$m.
- the absolute values of the unknown `zeroc[]` and `backc[]` corrections (Table 3 [p.9]) are bounded to about $200\,\mu$m.

If we accept these assumptions, then any range residual larger than about $600\,\mu$m is probably due to bad data, which we can delete for the second adjustment. Furthermore, all data which were given low weight in the initial filtering can also be deleted (we have seen their statistical summary, and don't need them anymore). These editing operations are implemented in the program which produces Table 6 [p.18]; it writes a new range data file, ready for input into Gaussfit:

	Processing "`bl2`" sort of `rfpcPlane4Data.gfp`	
2200	ranges processed by `rfpcPlane4AverageBl2`	
577	ranges deleted by Chauvenet criterion	*presumed outliers*
658	ranges deleted because $w < 4$ ($\sigma > 0.5$mm)	*done with them*
100	ranges deleted because $\lvert\Delta R\rvert > 0.6$mm	*presumed outliers*
865	ranges written by `rfpcPlane4AverageBl2`	

[11] An observation with $\sigma = 1\,$mm is given unit weight here.

baseline	r1	r2	n	iters	n'	$\overline{\Delta R}$ μm	$\sigma_{\overline{\Delta R}}$ μm	$\overline{A}$ mV	$\overline{R}$ m	$\sum w$ [σ = 1 mm]
1	101	102	70	5	65	-61	52	7865	62	20454
2	101	103	33		33	208	152	626	120	1017
3	101	104	69	56	13	515	33	1503	170	1700
4	101	105	69	27	42	61	90	1505	208	12502
5	101	110	36	6	30	22	64	1377	170	3819
6	101	111	59	57	1	-140	0	1269	120	400
7	101	112	36	2	34	-118	66	4223	62	4346
8	102	101	36		36	217	294	12441	62	36
9	102	104	36	7	29	114	40	11339	120	9306
10	102	111	36	13	23	35	45	10247	169	4412
11	102	112	36	6	30	196	41	10912	120	6015
12	103	101	69	60	9	175	25	1700	120	806
13	103	102	69	33	36	90	59	11053	62	8415
14	103	104	69	3	66	375	103	2645	62	4721
15	103	105	67		67	295	179	597	120	1566
16	103	106	36	2	34	-232	111	1136	170	5103
17	103	112	38	34	3	110	0	1231	170	372
18	104	101	69	40	29	-146	42	1549	170	7139
19	104	102	69	38	31	-254	125	1341	120	6337
20	104	103	33		33	-275	135	1044	62	2316
21	104	105	68	33	35	-234	93	11217	62	9212
22	104	106	69	14	55	200	134	1385	120	9046
23	104	112	39	6	33	-122	63	912	208	6127
24	105	101	36		36	-279	203	436	208	36
25	105	103	29	1	28	449	242	57	120	28
26	105	104	68	3	65	480	161	2600	62	65
27	105	106	66		66	499	213	4153	62	66
28	106	103	4	2	2	-1151	40	57	170	2
29	106	104	67	14	53	88	102	1242	120	6527
30	106	105	68	16	52	-237	73	1261	62	5444
31	110	101	36		36	-363	271	3983	170	36
32	110	111	36	2	34	-273	201	8624	62	34
33	110	112	36		36	-466	368	9651	120	36
34	111	101	36	34	1	-210	0	888	120	196
35	111	102	36	33	2	-370	0	1741	169	401
36	111	110	69	10	59	0	49	11628	62	12850
37	111	112	70	8	62	21	67	10612	62	8453
38	112	101	52		52	-1156	656	568	62	325
39	112	102	69		69	231	447	565	120	431
40	112	103	32		32	289	248	88	170	200
41	112	104	41	8	33	991	56	136	208	206
42	112	110	69		69	-290	250	857	120	431
43	112	111	69		69	27	142	3520	62	431
0	0	0	2200	226	1974	-7	193	5685	110	168305

Table 6: Mean residuals from initial adjustment, on per-baseline basis

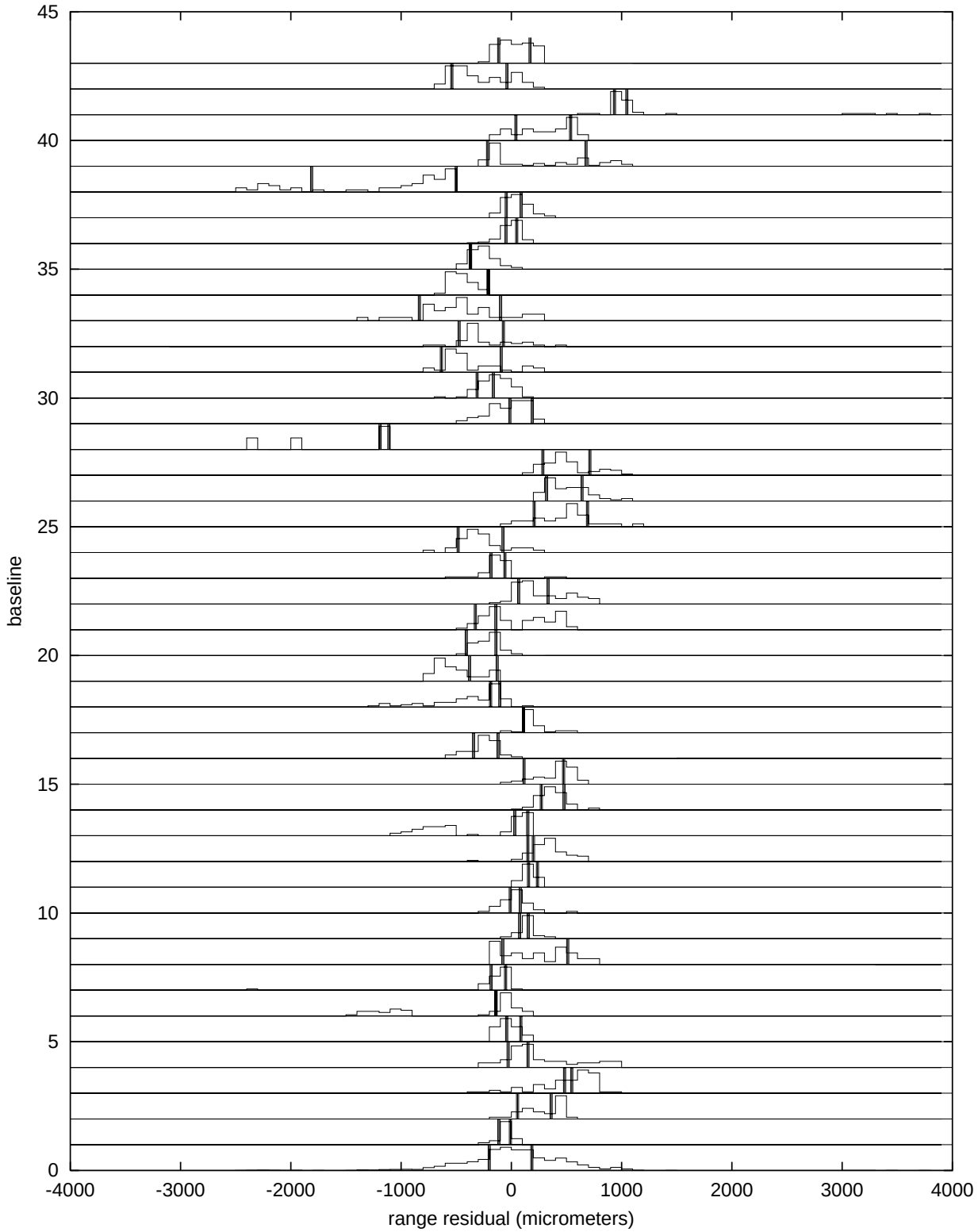

Figure 8: Histograms of range residuals per baseline (Table 6 [p.18]) after initial adjustment

Monument Adjustment					
ranger	axis	pr mm	$\sigma^2_{\mathtt{pr}}$	prc mm	$\sigma_{\mathtt{prc}}$ mm
101	0	16774.69	1	-0.08	0.02
101	1	118878.29	1	-1.10	0.04
102	0	73847.65	1	-0.19	0.02
102	1	94628.32	1	0.26	0.03
103	0	111273.88	1	-0.57	0.06
103	1	44936.98	1	-0.41	0.03
104	0	118818.20	1	-1.10	0.04
104	1	-16660.16	1	0.28	0.01
105	0	94562.73	1	-0.32	0.05
105	1	-73898.37	1	1.50	0.02
106	0	44964.99	1	0.66	0.10
106	1	-111244.72	1	1.05	0.09
110	0	-118783.07	1	0.10	0.16
110	1	16880.36	1	0.19	0.14
111	0	-94444.51	1	-0.02	0.06
111	1	74079.60	1	0.11	0.10
112	0	-44851.26	1	1.31	0.02
112	1	111355.86	1	-0.19	0.05

Table 7: Initial scan-point coordinates `pr[,]` and their second adjustment `prc[,]`

The filtered data file produced after the initial adjustment was then fitted by Gaussfit, using the same model and parameter files as in the initial adjustment. This produced a second set of adjusted monument corrections, which are shown in Table 7 [p.20]. Differences between the two solutions are of order 0.25 mm. The remarkably small formal errors of these adjustments to the Topcon survey coordinates are probably overoptimistic; the true errors are likely to be comparable to the unknown zero- and back-prism calibration corrections, perhaps of order 0.2 mm. In any case, it is likely that application of these corrections will improve the accuracy of the Topcon monument coordinates by 3× or more.

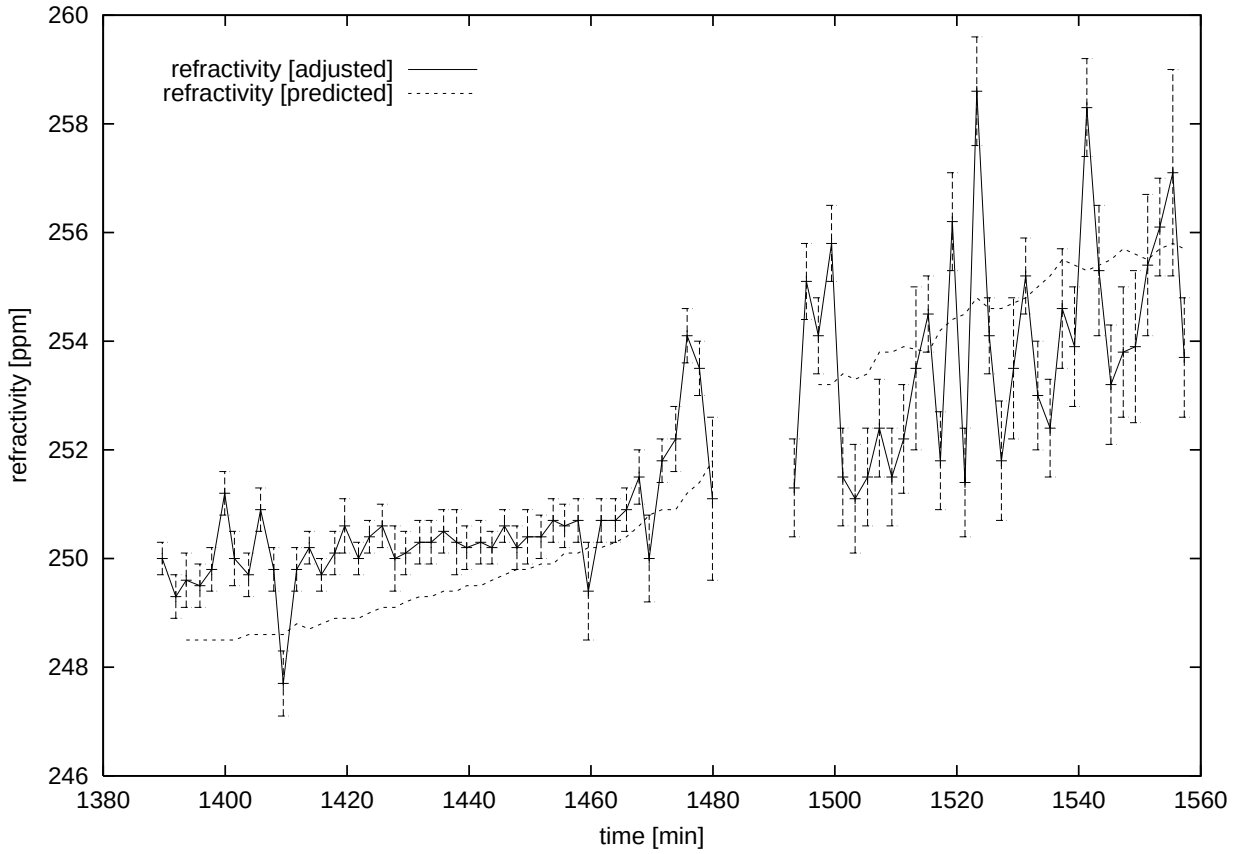

Figure 9: Refractivities estimated in second adjustment

The second set of adjusted refractivity corrections are shown in Figure 9 [p.21] (plotted with the adjustments added to the predictions), and are tabulated in Table 8 [p.22]. The predicted and observed refractivity variations plotted in Figure 9 [p.21] for the experiment are systematically different: observed is ≈ 1 ppm greater than predicted at first, and vice versa at the end. We can conjecture that the thermistors are in semi-equilibrium with their ventilated housings, and that those housings do not couple well to the air, and lag behind as air temperature changes. In addition to the systematic trend, the statistical properties of the predicted and observed curves are radically different: predicted refractivity is smooth (noise ≈ 0.1 ppm), whereas the observed refractivity shows somewhat impulsive events with amplitudes ≈ 5 ppm. One might be tempted to assume that isolated 2-minute cycles whose refractivity differs from the trend by several standard deviations are flukes, and should be ignored, or that such rapid changes in refractivity are unreasonable, and that the formal errors are overoptimistic. However, in a number of cases several successive cycles depart from the trend, and appear to be consistent to within their formal errors in doing so. It is also conspicuous that the impulsive behavior begins at about 1470 min (sunset?), exactly when the rate of change of temperature is at a maximum (Figure 5 [p.10]). These two facts suggest that maybe the variations are real, that we are observing convection cells. If we had more baselines and data of higher quality, and if we had the zero- and back-prism calibrations, we could try interpreting the residuals on each baseline as refractivity residuals versus time, and might detect moving patterns of refractivity change in the array of baselines. For the moment, Figure 9 [p.21] should be regarded as only a tentative hint of the types of refractivity variations which we might be studying in future analyses of rangefinder data.

Refractivity corrections for 2-minute scans								
scan	temp1 °C	temp2 °C	temp3 °C	dewpt °C	press mbar	refract ppm	refractc ppm	$\sigma_{\texttt{refractc}}$ ppm
101	0.0	0.0	0.0	0.0	0.0	254.0	-4.0	0.3
102	0.0	0.0	0.0	0.0	0.0	254.0	-4.7	0.4
103	22.7	23.6	23.6	9.3	925.8	248.5	1.1	0.5
104	22.7	23.3	23.9	8.8	925.8	248.5	1.0	0.4
105	22.7	23.5	23.6	9.6	925.8	248.5	1.3	0.4
106	22.7	23.6	23.4	9.6	925.8	248.5	2.7	0.4
107	22.6	23.6	23.7	9.6	925.8	248.5	1.5	0.5
108	22.7	23.4	23.5	9.5	925.7	248.6	1.1	0.4
109	22.5	23.3	23.5	9.1	925.7	248.6	2.3	0.4
110	22.5	23.4	23.5	9.2	925.8	248.6	1.2	0.4
111	22.5	23.2	23.6	9.3	925.7	248.6	-0.9	0.6
112	22.5	23.1	23.3	9.0	925.7	248.8	1.0	0.4
(Some lines omitted to fit page)								
202	0.0	0.0	0.0	0.0	0.0	254.0	1.1	0.7
203	18.6	17.8	17.2	10.1	926.1	253.2	0.9	0.7
204	18.3	17.9	17.2	9.9	926.1	253.2	2.6	0.7
205	17.3	17.9	17.4	10.2	926.0	253.4	-1.9	0.9
206	17.7	17.9	17.4	10.1	926.0	253.3	-2.2	1.0
207	17.7	17.7	17.5	10.3	926.0	253.4	-1.9	0.9
208	17.3	17.1	17.0	10.4	926.1	253.8	-1.4	0.9
209	17.3	17.1	17.0	10.4	926.1	253.8	-2.3	0.9
210	17.2	17.3	16.8	10.5	926.1	253.9	-1.7	1.0
211	16.6	17.2	16.8	10.3	926.2	254.0	-0.5	1.5
212	17.1	17.4	16.9	10.3	926.2	253.8	0.7	0.7
213	16.9	16.8	16.6	10.3	926.2	254.2	-2.4	0.9
214	16.9	16.5	16.2	10.6	926.2	254.4	1.8	0.9
215	16.6	16.5	16.1	10.7	926.3	254.5	-3.1	1.0
216	16.0	16.5	15.9	10.4	926.3	254.8	3.8	1.0
217	16.4	16.4	15.9	10.5	926.3	254.6	-0.5	0.7
218	16.6	16.4	16.0	10.5	926.3	254.6	-2.8	1.1
219	16.5	16.0	16.1	10.6	926.4	254.7	-1.2	1.3
220	16.2	16.0	16.1	10.5	926.3	254.8	0.4	0.7
221	15.6	15.9	16.0	10.6	926.4	255.0	-2.0	1.0
222	15.2	15.9	15.8	10.4	926.4	255.2	-2.8	0.9
223	14.8	15.6	15.8	10.3	926.4	255.5	-0.9	1.1
224	15.0	15.7	15.7	10.5	926.5	255.4	-1.5	1.1
225	15.3	15.7	15.7	10.2	926.5	255.3	3.0	0.9
226	15.3	15.3	15.7	10.4	926.4	255.4	-0.1	1.2
227	15.7	15.2	15.2	10.2	926.5	255.5	-2.3	1.1
228	14.7	15.5	15.3	10.2	926.5	255.7	-1.9	1.2
229	15.2	15.2	15.4	10.1	926.5	255.6	-1.7	1.4
230	15.4	15.2	15.4	10.1	926.5	255.5	-0.1	1.3
231	15.1	15.0	15.1	10.6	926.5	255.7	0.4	0.9
232	15.2	14.9	15.1	10.2	926.5	255.8	1.3	1.9
233	15.2	15.1	15.1	10.4	926.6	255.7	-2.0	1.1

Table 8: Temperatures and refractivity, second refractivity corrections solution

baseline	r1	r2	n	iters	n'	$\overline{\Delta R}$ μm	$\sigma_{\overline{\Delta R}}$ μm	$\overline{A}$ mV	$\overline{R}$ m	$\sum w$ [σ = 1mm]
1	101	102	58	1	57	-53	56	7985	62	20047
2	101	103	33	2	31	220	159	637	120	988
3	101	104	12	7	5	428	48	1576	170	1606
4	101	105	41	3	38	67	81	1508	208	11954
5	101	110	13	6	7	4	27	1535	170	2800
6	101	111	1		1	-170	0	1269	120	400
7	101	112	16		16	-160	69	4219	62	4328
8	102	104	24	1	23	102	37	11323	120	8901
9	102	111	11		11	34	45	10252	169	4400
10	102	112	15		15	178	45	10923	120	6000
11	103	101	2		2	125	5	1691	120	800
12	103	102	21	3	18	69	40	11103	62	7200
13	103	104	41	1	40	387	97	2665	62	4624
14	103	105	32	1	31	321	200	446	120	1481
15	103	106	33		33	-239	126	1136	170	5100
16	103	112	1		1	110	0	1215	170	370
17	104	101	21	3	18	-155	30	1556	170	6111
18	104	102	26	1	25	-240	132	1349	120	6241
19	104	103	25		25	-256	143	1039	62	2305
20	104	105	23	1	22	-206	87	11192	62	8800
21	104	106	37	6	31	140	56	1366	120	7519
22	104	112	33	2	31	-57	45	901	208	5612
23	106	104	45		45	94	110	1243	120	6514
24	106	105	22	3	19	-215	65	1279	62	5165
25	111	101	1		1	-190	0	888	120	196
26	111	102	1		1	-370	0	1739	169	400
27	111	110	32		32	4	53	11673	62	12800
28	111	112	21	1	20	9	60	10663	62	8000
29	112	101	11		11	-597	39	1763	62	69
30	112	102	48		48	-36	266	752	120	300
31	112	103	30		30	259	307	89	170	188
32	112	110	66		66	-253	268	838	120	412
33	112	111	69		69	25	153	3520	62	431
0	0	0	865	11	854	-8	181	5856	110	159932

Table 9: Mean residuals from second adjustment, on per-baseline basis

This second adjustment can also be analyzed to produce the mean residual and standard deviation for each baseline, and this is tabulated in Table 9 [p.23] and plotted in Figure 10 [p.24].[12] Many baselines in Table 9 [p.23] have $\sigma_{\overline{\Delta R}} < 100\,\mu$m but $|\overline{\Delta R}| > 100\,\mu$m, which implies that the results of this experiment are dominated by some major source of systematic error. *The simplest explanation for this observation is to conjecture that the not-yet-calibrated zero- and back-prism offsets are of order* ± 0.005 inch *(*$\pm 125\,\mu$m*).*

The single summary number which characterizes the whole experiment is the $\sigma_{\overline{\Delta R}}$ value for baseline "0" (last row of Table 9 [p.23]); it is the overall weighted RMS closure error. The number of ranges contributing to that RMS is given by the n' for baseline 0 (same row).

[12] Gaussfit contains a "robust estimation" capability [JFMM88, Sect.2.4]: the capability to automatically reject outliers. As an experiment, this second adjustment was tried with the Gaussfit environment variable `fair` set, which implements the "fair" non-Euclidean metric in the residuals [Rey83]. Gaussfit eventually converged to a solution, after about 50 iterations, but the solution it found had no obvious advantages over the conventional least-squares solution.

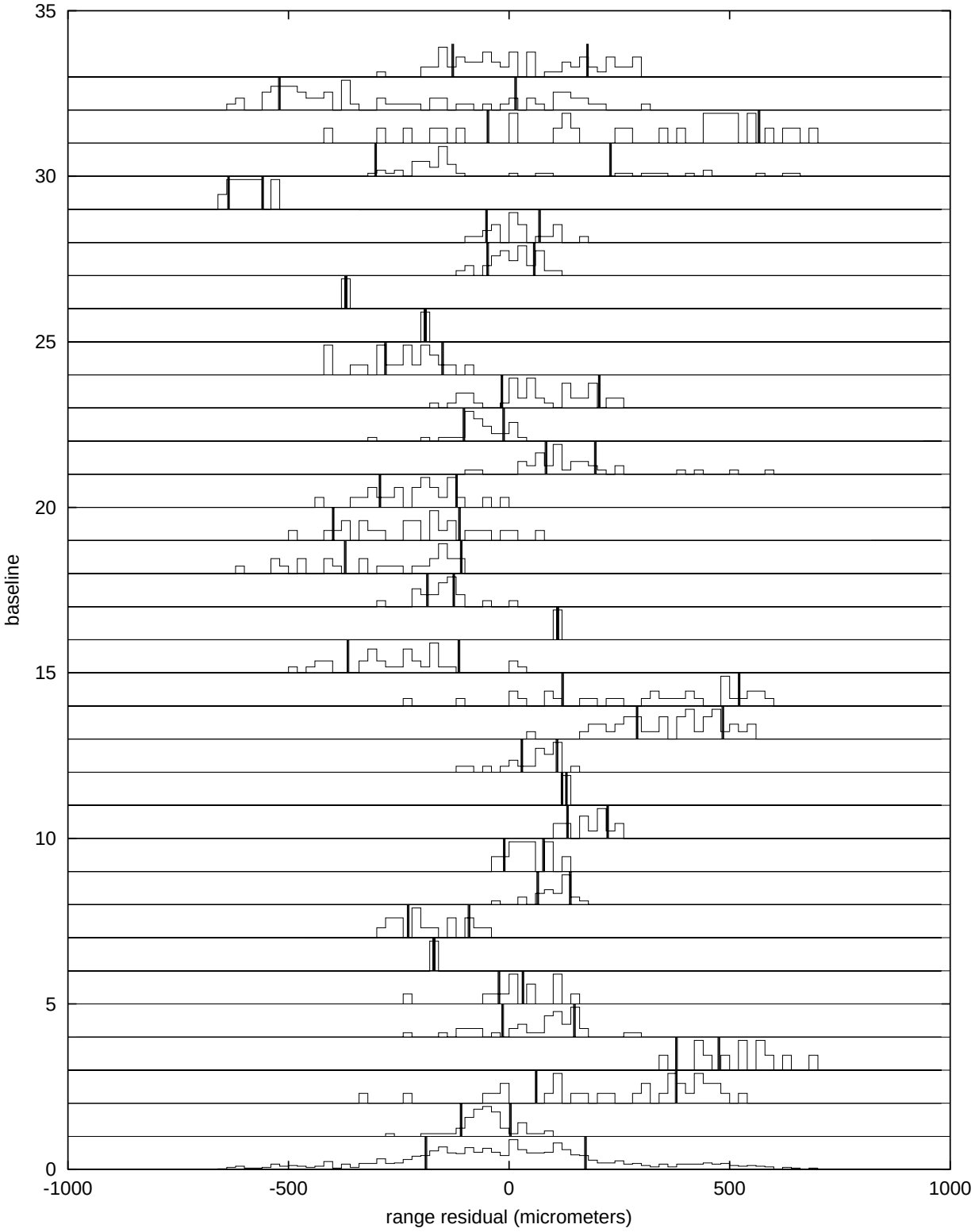

Figure 10: Histograms of range residuals per baseline (Table 9 [p.23]) after second adjustment

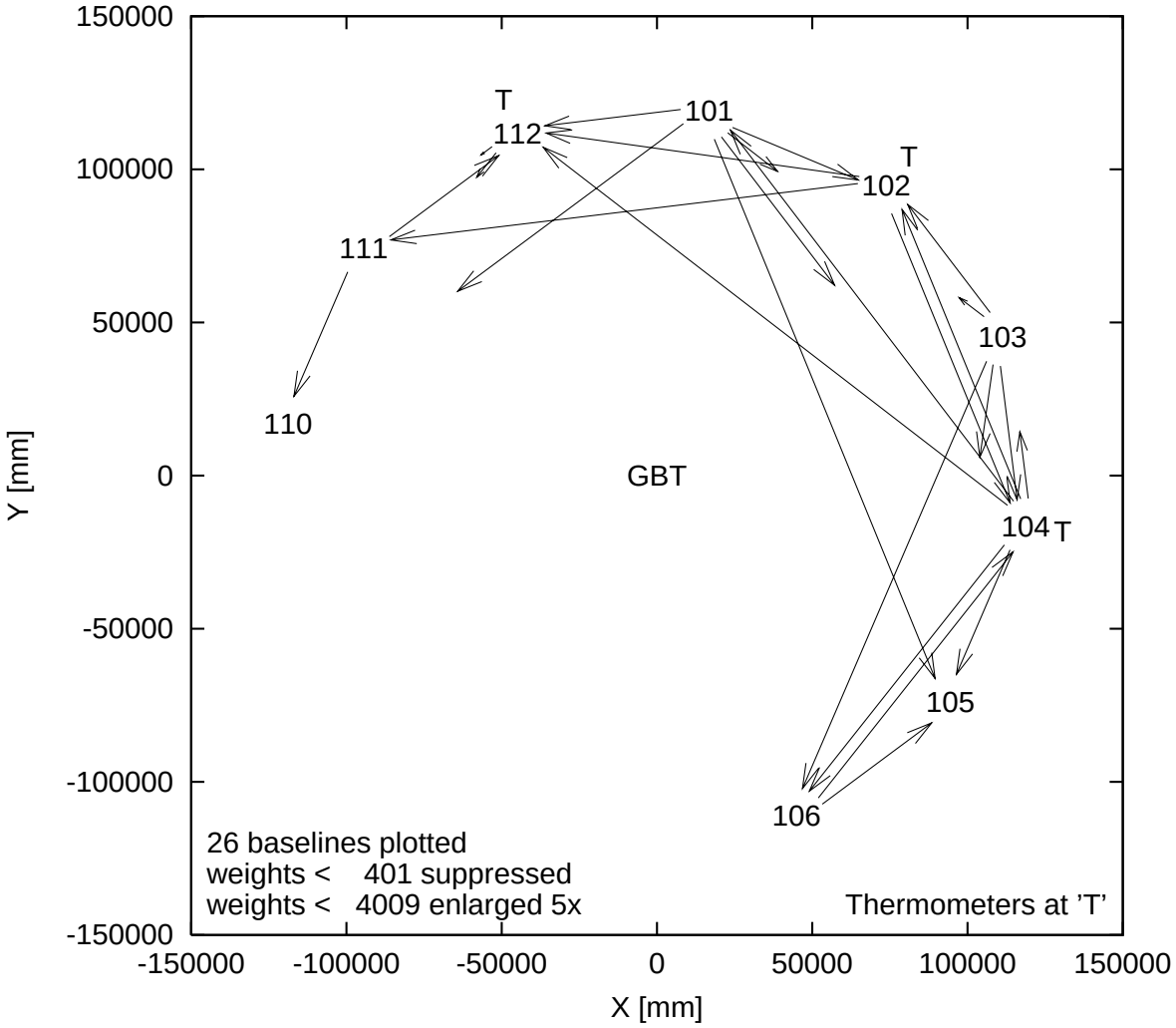

Figure 11: Geometry of weighted baselines (Table 9 [p.23]) after second adjustment

Figure 11 [p.25] shows the geometry of the baselines whose statistics are tabulated in Table 9 [p.23]. The fractional lengths of the vectors are proportional to the relative weights in Table 9 [p.23]. All baselines with 20% or more of the maximum weight are plotted with full-length vectors; baselines with less weight have proportionately shorter vectors. Baselines with less than 2% of the maximum weight are suppressed for this figure. The figure demonstrates that we have enough data to derive the monument and refractivity adjustments (with the assumption of nominal zero- and back-prism offsets), but we have only modest amounts of redundancy in the experiment after the filtering and iterative rejection operations have discarded so much data. In summary, we did indeed perform a phase closure experiment on 1999-06-23, but only *just barely*.

5 Conclusions & recommendations

There are two summary results of this work:

- The residuals from an adjustment of monument and refractivity corrections using ≈ 850 of the 5000+ ranges acquired 99-06-23 demonstrate that the total system of atmosphere plus GBT rangefinder hardware and software plus model-fitting analysis software achieved phase closure with a weighted RMS accuracy ≈ 180 μm. We conjecture that this accuracy was limited by a combination of rangefinder hardware problems which existed on 99-06-23 plus not-yet-calibrated prism offsets.

- The mean refractivity for the whole set of baselines can be determined to ≈ 1 ppm in *each* scan cycle. Refractivity changes determined this way generally agree with refractivity changes predicted from ambient air temperature to several ppm, but observed refractivity fluctuates more rapidly than does refractivity predicted from thermometer readings.

Recommendations for future work are:

- The monument coordinate corrections `prc[,]` tabulated in Table 7 [p.20] should be applied to the monument coordinates previously determined from the Topcon survey; they should reduce the survey errors from about ±1000 μm to perhaps ±200 μm.

- The zero and back prisms of the nine rangefinders should be calibrated, even if only in a provisional manner. For example, it should be possible to use a dial guage or some similar device to measure the faces of the zero- and/or back-prisms relative to the surrounding metal surface. The design intent was zero difference, but the as-built prisms probably deviate by about 0.005 inch from zero, and these unknown offsets are limiting our ability to achieve closure. It would even be useful to calibrate a subset of the rangefinders, or just the back-prisms, or just the zero-prisms; any such data with accuracy 0.002 inch or better will be likely to reduce the closure residuals in a simple adjustment, and may also improve our ability to infer unmeasured offsets from datasets with more redundancy.

- We need to perform one or more new phase-closure experiments in the plane, now that the instrumentation has been repaired and improved. Our goal is to demonstrate closure limited only by atmospheric and instrumental noise, at levels below 100 μm. It will be important to demonstrate that the monument coordinate corrections in Table 7 [p.20] are confirmed by future experiments.

- The next experiment should include at least one retroreflector in the plane which is visible from at least three rangefinders. This will verify the zero-prism offsets free from any uncertainty about back-prism offsets.

- Phase stability of the rangefinders should be monitored closely until causes of phase changes are better understood. Some recent tests have demonstrated range noise levels below 10 μm; for such instruments the phase change rates greater than 10 μm/min which were seen in the 99-06-23 experiment would be a limiting factor. If the rates cannot be reduced, ZRG sampling intervals should be shortened to 30 seconds or less.

- Saturation (too much signal) should be detected in the rangefinder firmware. Probably this should be implemented as a third-harmonic (3θ) measurement; if the ratio of third-harmonic amplitude to first-harmonic amplitude (from which the distances are estimated) is more than some threshold, it will indicate *clipping* of the signal.

- Leakage amplitude and phase should be measured periodically and should be subtracted (using complex arithmetic) from all other measured amplitudes and phases. In particular, the leakage should be subtracted from both target and ZRG amplitude plus phase separately, *before* ZRG phases are subtracted from target phases.

References

[AKW88] Alfred V. Aho, Brian W. Kernighan, and Peter J. Weinberger. *The AWK programming language.* Addison-Wesley, New York, 1988. QA76.73.A95A35, ISBN 0-201-7981-X.

[Cre98] Ramón E. Creager. The Green Bank Telescope laser metrology system ZIY version 2.5 software interface reference manual. GBT Memo 189, National Radio Astronomy Observatory, Green Bank, WV 24944, September 1998. This GBT Memo contains only the table of contents of the manual; complete copies can be obtained by requesting GBT Archive L0480 from `scurry@nrao.edu`. An earlier version of this manual was published in January 1994 as GBT Memo 111.

[Gol96] M. A. Goldman. GBT dish laser range measurement corrections. GBT Memo 154, NRAO, June 1996. "..range measurements.. must be adjusted to compensate for details of prism mounting geometry, when finding distances from the scan reference point to the dish surface.. correction equations are provided..".

[Gol98] M. A. Goldman. Dynamical rangefinder measurements. GBT Memo 188, NRAO, June 1998. "..problem of.. adjusting the measured ranges to give the coordinates of the target point's trajectory versus time.. velocity and acceleration.. determined.. by the commanded telescope pointing schedule.. Methods of range interpolation are presented. Range rate corrections to measured range distance are given".

[JFMM88] William H. Jefferys, Michael J. Fitzpatrick, Barbara E. McArthur, and James E. McCartney. *User's Manual—GaussFit: A system for least squares and robust estimation.* The University of Texas at Austin, 1.0-12/2/88 edition, December 1988. Gaussfit is a program which supports a full-featured programming language in which models can be built to solve generalized least squares (both linear and nonlinear) and robust estimation problems. Derivatives are computed analytically, linear constraints and orthogonal distance regression are supported and errors in independent variables and correlated observations are handled correctly. See also `ftp://clyde.as.utexas.edu/pub/gaussfit/` and `http://clyde.as.utexas.edu/Gaussfit.html`.

[Par61] Lyman G. Parratt. *Probability and experimental errors in science.* Constable (London) [Dover reprint 1971], 1961. Chauvenet criterion table appears on p.177.

[Par99] David H. Parker. Draft notes on the Green Bank Telescope laser metrology system. This unpublished and incomplete document has chapter titles "group refractive index", "laser pointing and tracking", "distance to coordinate calculations", "acoustic thermometry", "signal processing", "optics and mirror system", "calibration", "experimental data", "GBT architecture", "software" and "panel setting instrument", October 1999.

[Rey83] William J. J. Rey. *Introduction to robust and quasi-robust statistical methods.* Springer-Verlag, New York, 1983.

[WCS96] Larry Wall, Tom Christianson, and Randal L. Schwartz. *Programming Perl.* O'Reilly & Associates, Sebastopol, CA, second edition, 1996. QA76.73.P47W34, ISBN 1-56592-149-6.

[Wel99] Don Wells. Fitting models to simulated rangefinder data. GBT Memo 196, NRAO, March 1999. "Simulated rangefinder data is fitted to estimate rangefinder coordinates, zero points and backprism offsets, and to estimate coordinates of target retroreflectors. The translation and tilt of trusses with retroreflectors attached are estimated from rangefinder data, for the cases of differential backup-structure pointing corrections and subreflector pose determination..".